EEET ECOLOGICAL ENGINEERING & ENVIRONMENTAL TECHNOLOGY

Ecological Engineering & Environmental Technology, 2026, 27(9), 1–13
https://doi.org/10.12912/27197050/224467
ISSN 2719–7050, License CC-BY 4.0

Received: 2026.05.19
Accepted: 2026.07.31
Published: 2026.08.15

Highly efficient copper/clay catalysts for catalytic wet peroxide oxidation of methyl orange at circumneutral pH and ambient temperature

Omar Laidi[1*], Anass Omor[2], Fadile Abdelali[1], Chakir Boughaba[3], Karima Elkarrach[4], Mohammed Merzouki[1]

[1] Laboratory of Biotechnology. Environment, Agri-Food, and Health, Faculty of Sciences Dhar El Mahraz, Sidi Mohamed Ben Abdallah University, Fez, Morocco
[2] Laboratory of Electrochemistry Engineering, Modeling and Environment, Dhar El Mahraz, Sidi Mohamed Ben Abdallah University, Fez, Morocco
[3] Laboratory of Modeling and Simulation in Mechanics and Energetics (MSME), Faculté des Sciences, Université Mohammed V de Rabat, Morocco
[4] Department of Biology, Multidisciplinary Faculty, Cadi Ayyad University, 46000 Safi, Morocco
* Corresponding author's email: omar.laidi@usmba.ac.ma

ABSTRACT

This study focuses on the catalytic wet peroxide oxidation (CWPO) of the synthetic azo dye Methyl Orange (MO) using a set of clay-based catalysts impregnated with transition metals (Cu, V, Fe, and Mn). The prepared materials Cu/Clay, V/Clay, Fe/Clay, and Mn/Clay–were obtained through a wet impregnation route and characterized in detail using X-ray diffraction (XRD), scanning electron microscopy (SEM), and Fourier-transform infrared spectroscopy (FTIR) to elucidate their structural and surface properties. The degradation of MO was investigated under exclusive experimental conditions, including variations in catalyst loading, hydrogen peroxide concentration, and pH. Kinetic information indicated that the oxidation followed a pseudo–first order reaction. Among the examined catalysts, Cu/Clay exhibited the most efficient oxidative conduct, achieving approximately 98% color removal and nearly 70% reduction in chemical oxygen demand (COD) reduction after 3 h under optimized conditions (5% Cu loading, 4 g L^{-1} catalyst). The catalytic activity decreased in the following order: Cu/Clay > V/Clay > Mn/Clay > Fe/Clay. Overall, these effects suggest that copper-modified clays can function as sensible, low-cost, and environmentally sustainable catalysts for advanced oxidation processes (AOPs) to treat dye-contaminated wastewater.

Keywords: chemical oxygen demand; wastewater treatment; catalytic wet peroxide oxidation.

INTRODUCTION

Textile dyes, which are important synthetic chromophores in global manufacturing, pose a significant environmental legal responsibility in developing economies (Yanping and Dahlina Bt Rusli, 2024). The textile, brassware, and tannery industries in Morocco alone release approximately 10 million cubic meters of colored wastewater each year (Lamrani et al., 2026), flooding the receiving water bodies with this untreated wastewater. Ecotoxicological tests have validated their acute toxicity in microbial consortia, interference with aquatic photosynthesis, significant biotoxicity, and mutagenic and carcinogenic potential in scenarios of continuous exposure (Isibor and Imoobe, 2025). The complexity of effluents, caused by different types of dyes and chemical matrices, makes them even harder to degrade. Fragrant azo linkages and sulfonate substituents render them highly resistant to photodegradation and oxidation (Vaiano and De Marco, 2023). Standard remediation portfolios that include adsorption, coagulation/flocculation, membrane filtration and biotreatment are not always effective (Pessoa, 2025). Sorbent-based methods produce hazardous

stable waste, osmotic methods become fouled, and anaerobic digestion often produces carcinogenic aromatic amines that persist longer than the parent dyes (Shindhal et al., 2020).

Catalytic wet peroxide oxidation (CWPO) changes the game by turning biorefractory dyes into CO_2, H_2O, and inorganic residues or harmless intermediates under normal conditions (ambient T/P) (Azimi et al., 2020). Essentially, redox-active transition metals (Fe^{2+}, Cu^{+}, and Mn^{2+}) activate H_2O_2 to form hydroxyl radicals (-OH; E_0=2.80 V/NHE). These radicals are highly reactive ($k \approx 10^9$ $M^{-1}s^{-1}$) and can break C=C, N=N, and C-S bonds without care.

Published benchmarks highlight the divergence between catalysts. Contreras Olivares et al., 2016, attained 99% Reactive Black 5 decolorization via Fe(III)/Montmorillonite K10, while Yang and Yang, 2022 confirmed 4-chlorophenol mineralization over Al-Fe-Cu-pillared clays, crediting layered aluminosilicates for metal stabilization and mass transfer enhancement. Clay appeal stems from intrinsic attributes: high cation change potential (80–150 meq/100 g), lamellar structure amenable to pillaring, and price-effectiveness. However, homogeneous Fe-Fenton systems and early heterogenized variations remain pH-confined (optimum ≈3) to suppress $Fe(OH)_3$ gelation, rendering them impractical for native textile streams (pH 6-10) (Sun et al., 2018).

Cu (I/II) ($E°$= 0.17 V), Mn (II/III/IV), and V (IV/V) redox manifolds are non-ferrous options that do not require acidic conditions for their operation. They continue to produce -OH even under neutral conditions (Biswal and Ranjan, 2025). Mechanistic details are most important: copper speeds up the direct reduction of H_2O_2; manganese helps form surface peroxo-complexes; and vanadium activates Lewis acid, which changes the effectiveness, selectivity, and leaching oxidants (Oh et al., 2019).

This study addresses significant deficiencies by evaluating natural clay-derived catalysts (Cu/Clay, V/Clay, Mn/Clay, and Fe/Clay) for MO CWPO, an anionic azo probe (λ_{max}=464 nm) suitable for textile applications, using H_2O_2 at 293 K/1 abm. The synthesis included wet impregnation (metal nitrates, 0.5.5 wt% loading), selective thermal activation (300-500°C), and multiscale validation: XRD (phase registry), SEM/EDX (morpho-dispersion), FTIR (M-O coordination), and textural analysis (BET) and leachability profiling (ICP-MS). Operational mapping systematically separated pH (3–9), catalyst dosage (0.5–4 g/L), and $[H_2O_2]_0$ (5–100 mM), resulting in pseudo-first-order kinetics ($r^2 \geq 0.98$) and mineralization metrics (color/COD/TOC). Cu/Clay was the best, with 98% decolorization and 70% COD abatement (pH 6.5, 3h) and less than 2% steel lixiviation over five cycles. This was better than the Fe (30%), Mn (79%), and V (80%) homologue. These results change the clay-based AOP layout by placing pH-strong, recyclable non-Fe catalysts at the top of the list for large-scale use in the textile effluent crisis in Morocco. This connects the promise of the laboratory to the practicality of business.

EXPERIMENTAL

Chemicals and reagents

Copper(II)nitratetrihydrate($Cu(NO_3)_2 \cdot 3H_2O$), ammonium metavanadate (NH_4VO_3), iron(III) chloride hexahydrate ($FeCl_3 \cdot 6H_2O$), manganese (II) nitrate tetrahydrate ($Mn(NO_3)_2 \cdot 4H_2O$), hydrogen peroxide (30 wt%), and Methyl Orange (MO) have been procured from Sigma-Aldrich and used as received (analytical grade, no similarly purification).Ultrapure water was obtained from a Milli-Q Direct-Q UV3 machine (resistivity 18.2 MΩ·cm).

Catalyst preparation

Moroccan bentonite clay was used as a guide, and its bulk composition was determined by X-ray fluorescence (XRF): SiO_2 (37.86 wt.%), Al_2O_3 (10.43 wt.%), Fe_2O_3 (4.65 wt.%), MnO (0.06 wt.%), MgO (2.52 wt.%), CaO (18.72 wt.%), Na_2O (0.26 wt.%), and K_2O (2.34 wt.%) (Marouf et al., 2021). The raw clay was purified by repeated washing with ultrapure water to remove soluble impurities, followed by overnight drying at 100 °C.

Clay-supported metallic oxide catalysts were synthesized via wet impregnation. Metal precursors were dissolved (focused on 1.5–7.5 wt.% metal loading) in 50 mL distilled water. The clay powder was suspended in the solution and stirred vigorously (120 rpm) in a 100 °C water bathtub until the entire solvent evaporated. The dried solids (105 °C, overnight) underwent calcination at 500 °C for 4 h (5 °C/min ramp, muffle furnace) to join the active levels.

Catalyst characterization

The crystalline stages were identified using powder X-ray diffraction (XRD) on a Panalytical X'Pert PRO diffractometer (Cu Kα radiation, λ = 0.154060 nm; 40 kV, 30 mA; 2θ = 10°–80°; 0.017° step, 1 s/step).

Morphology and elemental mapping were performed using scanning electron microscopy-energy dispersive X-ray spectroscopy (SEM-EDX) (FEI Quanta 200 FEG, 15–20 kV, EDAX detector).

Surface functional groups and metallic-clay interactions were probed using Fourier-transform infrared (FTIR) spectroscopy (Bruker Vertex 70, 400–4000 cm^{-1}, 4 cm^{-1} resolution, KBr pellet).

The clay bulk composition was quantified using XRF (PANalytical Axios, wavelength-dispersive, Be–U).

Catalytic activity evaluation

Batch CWPO experiments were performed to assess MO degradation (C_0 = 4.6 × 10^{-5} mol/L, 50 mL) at 25 °C in a 100 mL glass reactor. The catalyst (optimized dose) was dispersed inside the dye solution and stirred magnetically (400 rpm, 15 min) to reach adsorption-desorption equilibrium. H_2O_2 was then modified and dosed, marking t = 0.

Post-response aliquots were filtered (0.45 µm syringe filters) to quench the catalysis and isolate the particulates from the solution. Decolorization was quantified spectrophotometrically (Jasco V-530, λmax = 464 nm) for 180 min. Blank runs (without the catalyst) showed negligible abiotic decay.

Parametric studies optimized pH (3–9, adjusted using 0.1 M HCl/NaOH), catalyst loading (0.5–4 g/L), and [H_2O_2]$_0$) (5–100 mM). The MO elimination performance (%) was calculated as follows:

$$Decolorization\ efficiency\ (\%) = \left[\frac{C0 - Ct}{C0}\right] \times 100 \quad (1)$$

where: $C0$ is the initial attention of the dye solution, and Ct is the attention of the dye solution at time t.

The chemical oxygen demand (COD) was measured using a COD meter (HACH COMPANY) after a response time of 1 h, and the COD removal performance was calculated using the following equation:

$$COD\ removal\ efficiency\ (\%) = \left[\frac{COD\ initial - COD\ final}{COD\ initial}\right] \times 100 \quad (2)$$

RESULTS AND DISCUSSION

XRD results

Figure 1 shows the XRD pattern of the clay. The dominant crystalline phases observed in the clear diffractogram appeared at 2θ angles of 20.9°, 26.7°, and 29.4° and were attributed to calcite and quartz, respectively.

The XRD profiles (Figure 2) of all the catalysts exhibited diffraction peaks similar to those of pure clay, 2θ = 26.7°, indicating that the structural framework was preserved even after incorporating metal oxides. However, the diffractograms of the catalysts showed the emergence of new phases in the XRD patterns. In the Cu/Clay catalyst, the most intense peaks, attributed to the characteristic reflections of crystalline CuO (Minyukova et al., 2018), appeared at 35.45° and 38.6°, respectively. In the Mn/Clay catalyst, the MnO_2 phase was observed with peaks at 37.3°, 42.6°, and 56.6°, respectively. Several vanadium crystalline sources were detected in the V/Clay catalyst. Indeed, some reflections from the vanadium-containing phases (mainly at approximately 20°, 26°, and 30°) overlapped with the reflection angles characteristic of the host mineral and quartz impurity (Duchesne et al., 2016). The peaks attributable to V_2O_5 appear at approximately 20.2°, 26.09°, and 30.98° (Gaibnazarov et al., 2023). All samples presented typical oxide profiles, indicating that most of the metal oxides were immobilized in the clay through the impregnation method.

SEM results

The surface morphology of the raw clay sample was examined using Scanning Electron Microscopy (SEM), and the results are presented in Figure 3. This reveals a uniform distribution of particles, associated with a high BET-specific surface area of 58 m^2/g and an exceptional adsorption capacity for various substances. The EDX spectrum further confirmed the presence of the major elements previously identified by X-ray

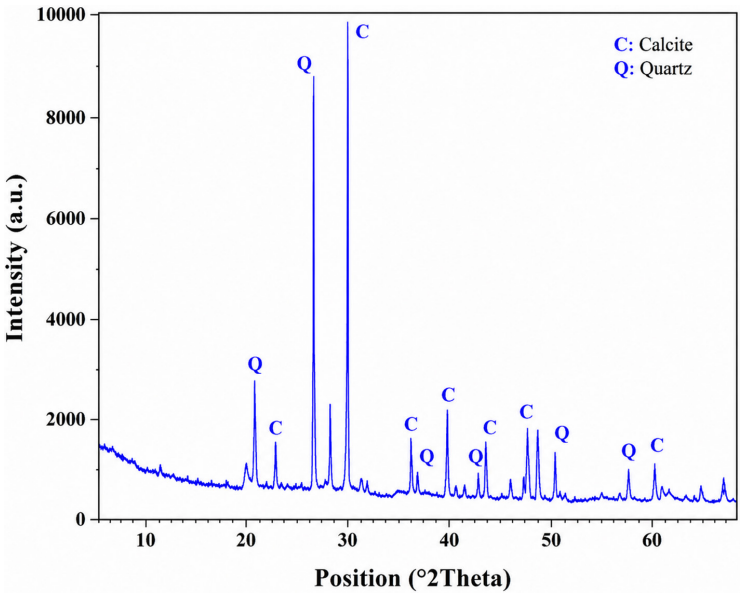

Figure 1. X-ray powder diffraction pattern of raw Clay

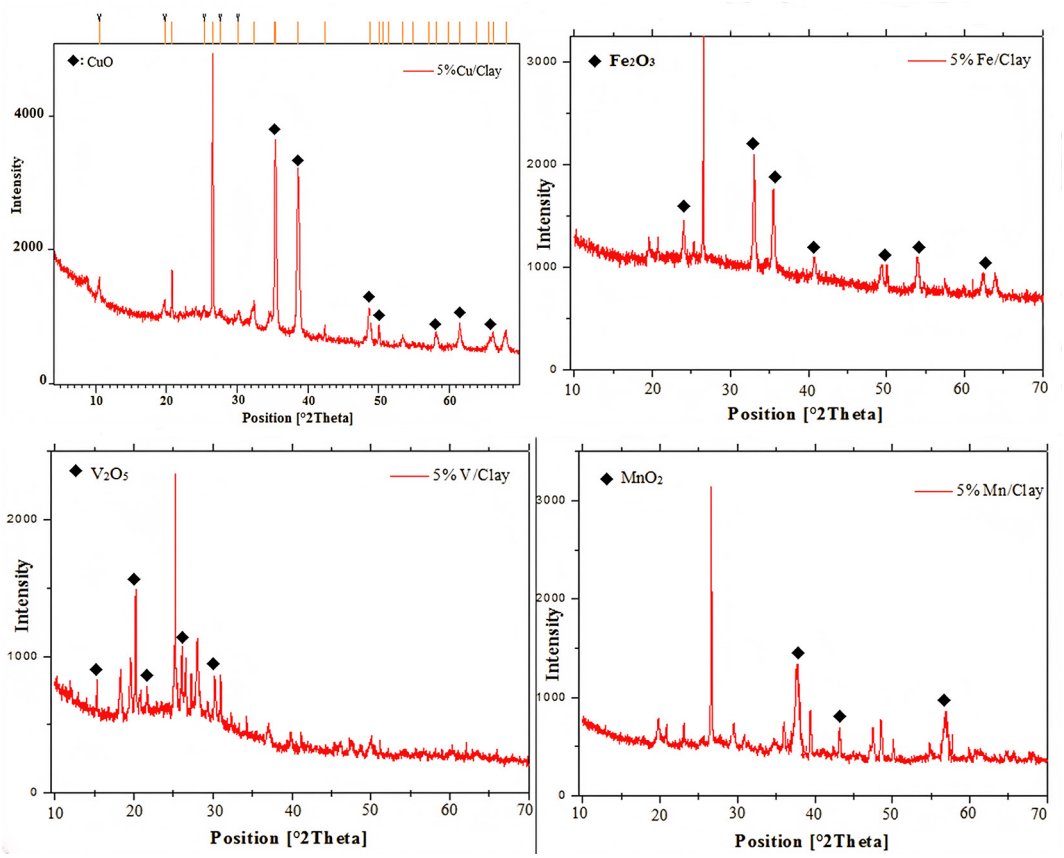

Figure 2. XRD patterns of calcined catalysts, 5% Cu/Clay, 5% V/Clay, 5% Mn/Clay and 5% Fe/Clay

fluorescence (Si, Al, Na, Mg, Ca, and Fe), thus validating these results. However, impregnation with metal oxides significantly alters the surface morphology (Ichikawa and Nakamura, 2023). The samples intercalated with copper and vanadium oxides were distinguished by cornflake-like crystals with a fuzzy appearance, indicative of their particularly fine lamellar structures (Rajesh Ch and Rao N, 2022). This change can likely be attributed to the reduction in the initial amorphous phases and modification of the surface charge induced by the chemical process.

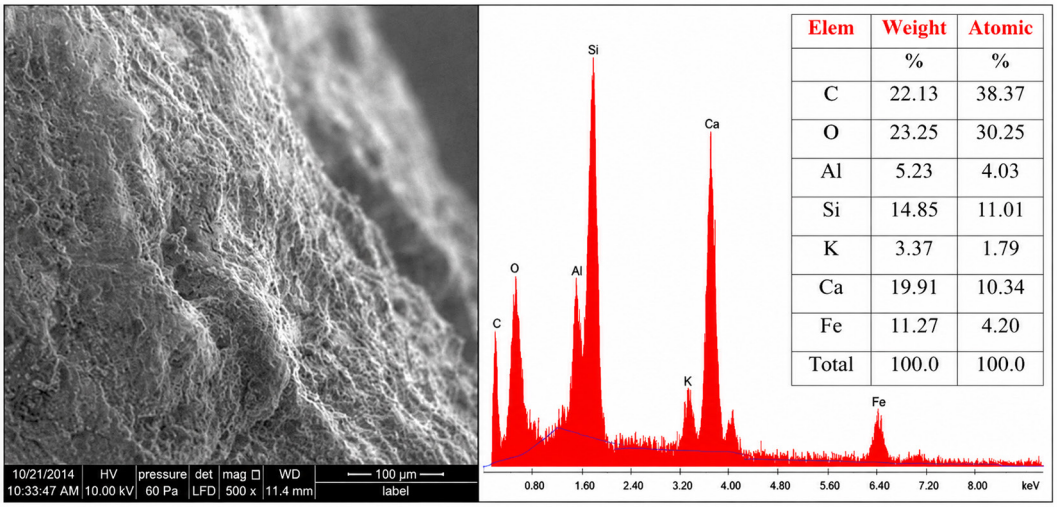

Elem	Weight %	Atomic %
C	22.13	38.37
O	23.25	30.25
Al	5.23	4.03
Si	14.85	11.01
K	3.37	1.79
Ca	19.91	10.34
Fe	11.27	4.20
Total	100.0	100.0

Figure 3. SEM images coupled by EDX of Clay

In contrast, the samples impregnated with Fe and Mn (Figure 4c, d) displayed a more massive and irregular appearance, characteristic of a homogeneous dispersion of oxides across the entire surface of the clay (Van Groeningen et al., 2020), as confirmed by XRD. Finally, EDX analysis of the four catalysts confirmed the presence and excellent distribution of metals (Cu, Fe, Mn, and V) compared to the native clay.

FTIR results

The FTIR spectra (4000–400 cm^{-1}) of all the samples are shown in Figure 5. The persistence of all characteristic bands of the clay structure in the samples indicates that the host mineral remained intact after metal impregnation. In the O–H stretching region, the distinctive bands at 3620, 3653, 3690, and 3400 cm^{-1} correspond to the Al–OH groups, with an absorption at 3600 cm^{-1} associated with the internal hydroxyl groups located between the tetrahedral and octahedral sheets of the clay mineral. The OH bending band at 1630 cm^{-1} confirms the presence of hydration water linked to pillaring. The intense peaks at 1415 cm^{-1} are attributed to freely bound water molecules due to the hydration effects induced by metal pillaring. The typical Si–O–Si stretching bands, located at approximately 1001 cm^{-1}, exhibited a slight shift towards lower frequencies after impregnation, with no significant change in intensity. The lower-intensity bands at approximately 505, 693, 789, and 872 cm^{-1} correspond to the Al–O–Si, Si–O, Al–OH, and Al–OH–Al bonds, respectively, in the clay structure.

Compared to the native clay, the FTIR spectra of the catalysts show minimal changes, except for Cu/Clay, which reveals a new distinctive band at 1388 cm^{-1}, attributed to the Cu–OH bond, confirming the successful intercalation of copper into the clay (Kloprogge et al., 2021). The signals for the V–OH species at approximately 3650 cm^{-1} likely overlap with those of the hydrogen-bonded silanols in all the impregnated samples, whereas the intensity of the interlayer water band at 3410 cm^{-1} decreases. Finally, no significant metal oxide bands were detected in the spectra of the Fe/Clay and Mn/Clay catalysts, suggesting that the metal oxide particles were below the FTIR detection limit of the instrument (Hess, 2021).

Discoloration experiments

The effect of metal loading in the catalyst

Figure 6 presents the findings from the experiment with the catalysts Cu/Clay, Fe/Clay, V/Clay, and Mn/Clay, varying their metal loadings from 1.5, 2.5, 5, to 7.5 at.%. The results show a strong dependence of the catalytic activity on the metal ion concentration, with the maximum activity being 5% loading, with the results being 94% Cu/Clay, 65% V/Clay, 60% Mn/Clay, and 20% Fe/Clay. The activity of Cu/Clay can be attributed to the high redox potential of Cu_2^+/Cu^+ species as well as a strong coating of the clay, which can facilitate the rapid transfer of electrons, which in turn increases the formation of radicals that are responsible for the degradation of MO.

A 5% metal loading was optimal for the catalysts, as with higher loading (>5%), the activity

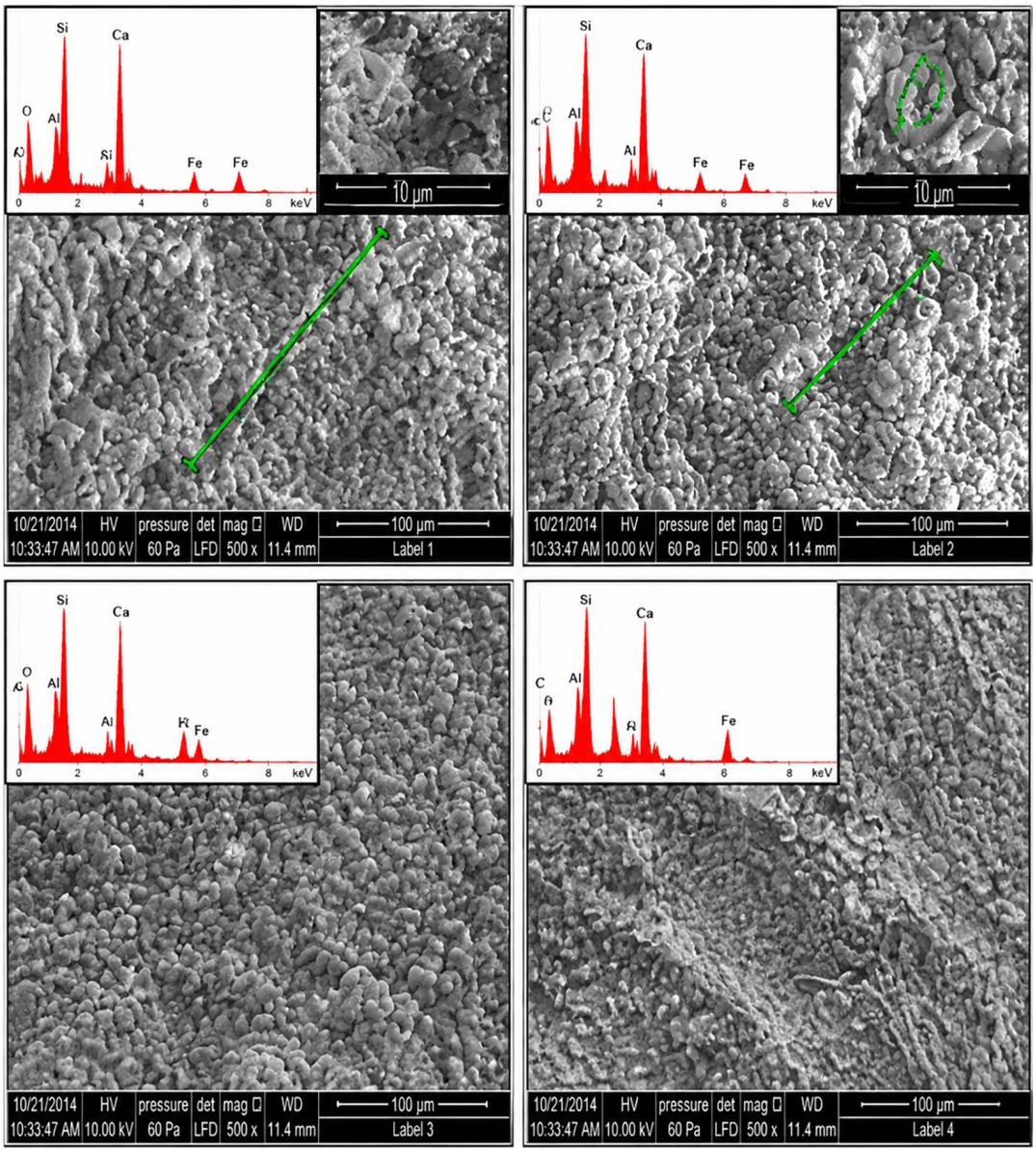

Figure 4. SEM Microscopy images coupled by EDX of (a)5%Cu/Clay, (b)5%V/Clay, (c)5%Mn/Clay and (d)5%Fe/Clay

decreased for Cu/Clay and Mn/Clay, while the rest of the catalysts remained unchanged. This is likely due to an overloading of the catalysts, which can initiate undesirable side reactions that can consume the OH– ions, which are considered the most important in MO decolorization to reduce the formation of metal hydroxides (Cu, Fe, V, Mn).

Effect of catalyst loading

Figure 7 shows the effect of catalyst amount on methyl orange (MO) decolorization. In heterogeneous Fenton-like systems, the reaction between ferrous or non-ferrous ions and hydrogen peroxide occurs in close proximity to the catalytic base, making it highly dependent on the exact base area of the material (Enami et al., 2013). It also promotes the formation of hydroxyl radicals (Raza et al., 2023).

The experiments were performed under the following conditions: initial pH = 6 and H_2O_2 (30%) = 2.5 mL. When the Cu/Clay and Fe/Clay catalyst dosages were improved from one hundred and fifty mg to 200 mg, the decolorization efficiency slightly improved from 91% to 94% and from 23% to 28%, respectively. and rose to 63%. This improvement can be attributed to the increased availability of organic network sites on the catalytic substrate, which promotes the formation of free hydroxyl radicals (Mccann and

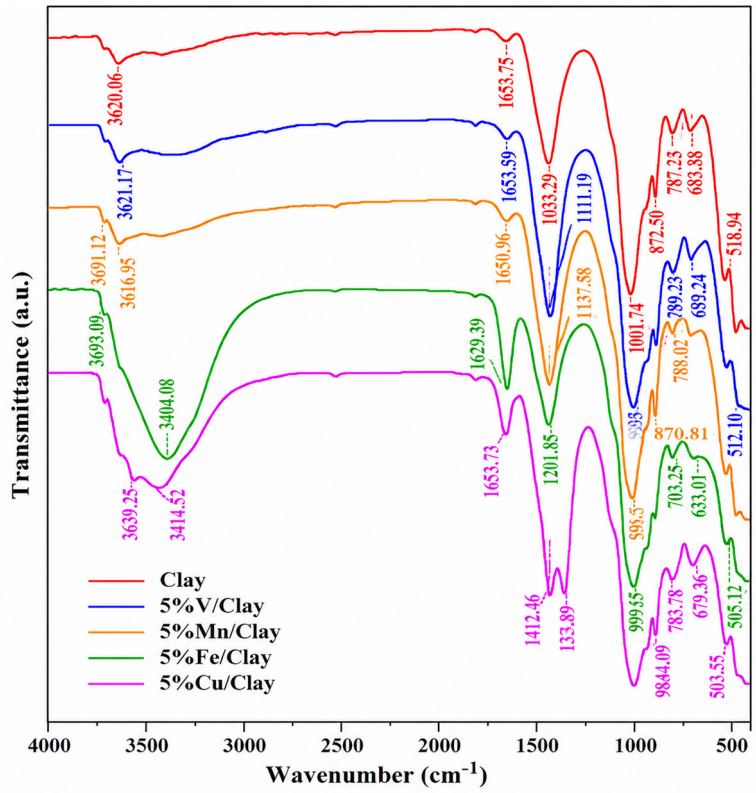

Figure 5. FTIR spectra of the Clay and the catalysts (5% Cu/Clay, 5% V/Clay, 5% Mn/Clay and 5% Fe/Clay)

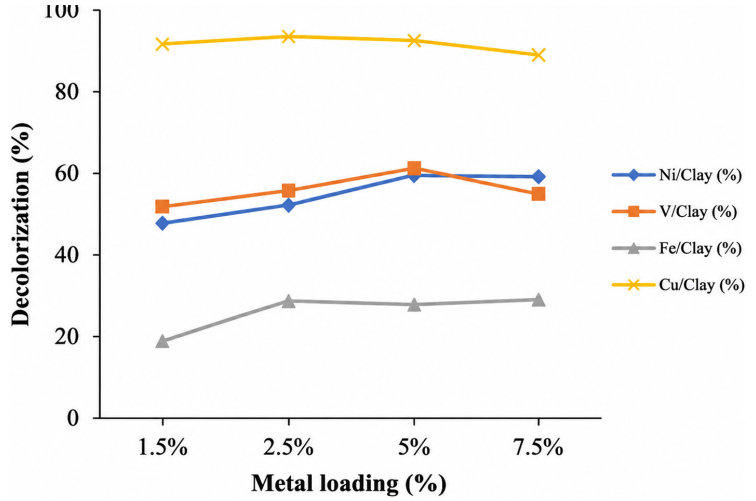

Figure 6. Decolorization efficiency as a function of metal loading for Cu/Clay, Fe/Clay, V/Clay, and Mn/Clay catalysts, obtained under well-defined reaction conditions (2.5 mL of H_2O_2, catalyst dosage of 200 mg, reaction time of 120 min)

Stahl, 2015). These reactive species effectively reduced the size of the dye chromophore, thereby improving the overall decolorization efficiency of methyl orange. However, the performance of all catalysts decreased when the catalyst loading exceeded 200 mg. This decrease is likely related to radical-radical recombination and excessive hydroxyl radical scission, both of which reduce radical availability and normal catalytic efficiency (Leifert and Studer, 2019).

Influence of hydrogen peroxide concentration

The concentration of hydrogen peroxide is a key parameter in Fenton-type processes because it governs the generation of reactive radical species responsible for the decolorization of dyes

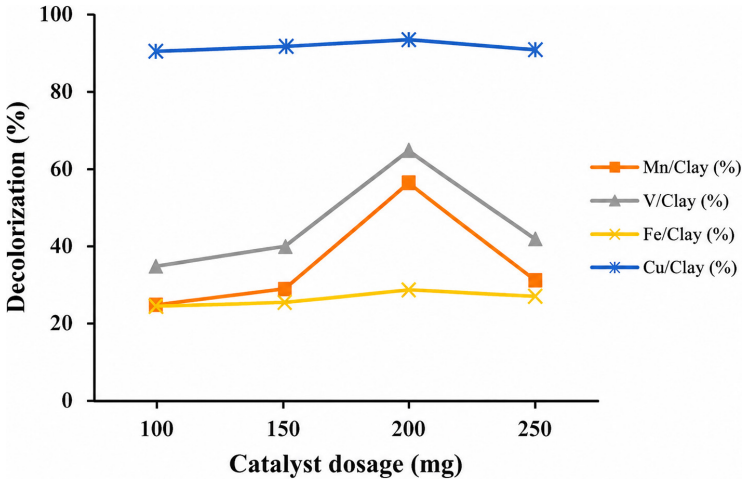

Figure 7. Influence of catalyst dosage on the decolorization efficiency of methyl orange (MO), obtained under well-defined reaction conditions (2.5 mL of H_2O_2, 5 wt% metal loading, and a reaction time of 120 min)

(Diya'Uddeen et al., 2012). The precise mechanism by which dyes are broken down in the presence of H_2O_2 is still under discussion. It is most likely that the process follows an adsorption-oxidation-desorption sequence. Initially, the dye molecules and H_2O_2 were adsorbed onto the catalyst surface. H_2O_2 is then broken down into highly reactive radical species, such as O_2^-, HO^-, and HO_2^-, through the catalytic action of the active sites of a solid catalyst (Pędziwiatr et al., 2018). These newly formed radicals possess strong oxidizing power and induce destructive oxidation of the organic dye. Finally, the low-molecular-weight degradation products obtained are desorbed from the catalyst surface, thereby regenerating the active sites (Hutchings, 2021). Figure 8 illustrates the influence of the amount of H_2O_2 on the oxidation of methyl orange (MO) dye molecules on the four catalysts, studied at different H_2O_2 concentrations (2–3 mL) while keeping the catalyst dosage (200 mg), initial dye concentration (15 mg/L), and contact time (120 min). It was observed that an increase in the molar amount of H_2O_2 accelerated the decolorization process for all four catalysts. For example, when the volume of H_2O_2 was increased from 2 to 2.5 ml in the case of Cu/Clay, the MO degradation efficiency increased from 85% to 91%. The catalytic performance of the prepared catalysts followed the order Fe/clay < Mn/clay < V/clay when 2.5 ml of H_2O_2 was used.

As mentioned above, hydrogen peroxide decomposes on the catalyst surface to generate hydroxyl radicals (Pędziwiatr et al., 2018). Therefore, higher concentrations of H_2O_2 can produce a greater number of hydroxyl radicals (Ros, 2021). However, the decolorization efficiency did not increase proportionally to the amount of H_2O_2 applied. When the volume of H_2O_2 was increased from 2.5 to 3 ml, the decolorization efficiency decreased from 63% to 47% and from 60% to 54% for V/Clay and Mn/Clay, respectively. This behavior is likely attributable to an excessive concentration of peroxides, in which hydroperoxyl radicals (HO_2^-) are formed from the hydroxyl radicals already generated (Eq. 3). Hydroperoxyl radicals are significantly less reactive and do not contribute significantly to the oxidative degradation of organic substrates, which occurs mainly through reactions with HO*(Mancipe et al., 2025).

$$H_2O_2 + HO\bullet \quad H_2O + HOO\bullet \qquad (3)$$

Consequently, 2.5 ml was the optimal amount of H_2O_2 for the decolorization of the dye on the four catalysts.

Influence of initial pH

Fenton-type reactions are highly dependent on the solution pH during oxidation. Although the conventional Fenton system achieves high oxidation efficiency, it operates effectively only within a narrow pH range (pH < 3.0), which is necessary to prevent the precipitation of Fe^{2+} and Fe^{3+} species in the reaction system (Chen et al., 2021). This constraint considerably limits the practical applicability of the conventional homogeneous Fenton process. Heterogeneous Fenton-type catalysts have been extensively studied to address this limitation.

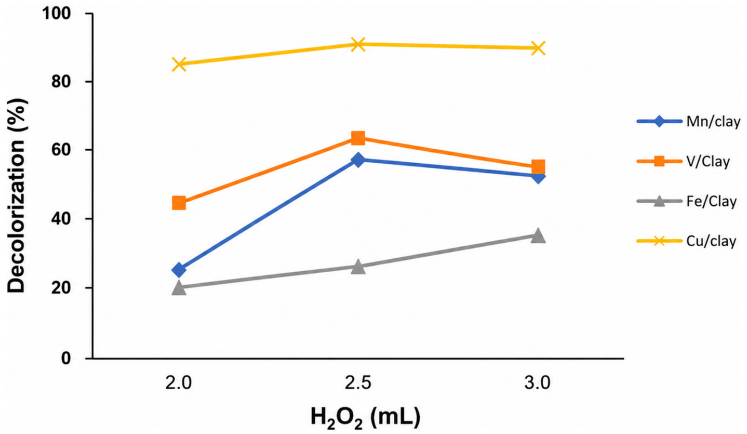

Figure 8. Effect of the initial hydrogen peroxide dose on the efficiency of methyl orange (MO) decolorization, obtained under well-defined reaction conditions (catalyst dose of 200 mg, metal loading of 5% by weight and reaction time of 120 minutes)

The influence of the initial pH on the removal of MO was investigated in the pH range of 3.0–7.0, without any subsequent pH adjustment during the experiments. Figure 9 shows that as the pH increased from 3 to 7, the decolorization efficiency of the V/Clay and Mn/Clay catalysts decreased; however, both catalysts still exhibited relatively high decolorization at pH 6 (~ 60.3% and 60.1% of MO was decolorized, respectively). The Fe/Clay catalyst achieved the highest decolorization efficiency of approximately 55% at pH 3. This aligns with the commonly accepted understanding that the ideal pH for traditional Fenton oxidation is between 2.5 and 3.5 (Pliego et al., 2015). Additionally, the catalytic effectiveness of Cu/Clay varied with the initial pH of the dye solution. Under these circumstances, a maximum decolorization efficiency of approximately 98% was achieved at a pH of 6, demonstrating that Cu/Clay maintains high activity over a much broader pH range. This indicates that Cu/clay can be effectively utilized under near-neutral conditions, significantly increasing its practical applicability for wastewater treatment in real-world applications (Pareek and Ledwani, 2022). Consequently, further experiments were conducted at pH 6, which corresponds to the natural pH of methyl orange solutions.

Catalytic performance and kinetic study

This study aimed to examine and evaluate the potential applications of four distinct catalysts in the oxidation of MO. One of the primary benefits of MO, an anionic dye, is that it does not adhere to the surfaces of any of the four catalysts at its natural pH, thus preventing interference from surface interactions during the reaction. Initial tests with MO in aqueous solutions and different catalysts specifically Cu/clay, V/clay, Mn/clay, and Fe/clay – verified that no adsorption occurred under the given experimental conditions. This property also facilitates the easy use of spectrophotometric monitoring at 464 nm to observe the progress and kinetics of reactions.

Decolorization and mineralization experiments were performed using 4.6×10^{-5} mol/L of MO dissolved in ultrapure water, and the results are shown in Figure 9. Over a 120-minute reaction period, the Cu/clay catalyst showed the highest activity, achieving a maximum decolorization of 91.67% and a chemical oxygen demand (COD) removal of 70%. In comparison, the COD removal efficiencies of V/clay, Mn/clay, and Fe/clay were 75%, 70%, and 20%, respectively, respectively. These findings highlight the superior oxidative performance of Cu/clay, underscoring its promising potential for dye degradation under moderate conditions of temperature and pH.

As shown in Figure 10, the general catalytic performance of MO oxidation on specific catalysts systematically changed after 180 min of reaction. In the presence of H_2O_2, the results showed that every catalyst tested showed measurable activity in MO oxidation.

Under the experimental conditions of natural pH and room temperature, the V/Clay and Mn/Clay catalysts exhibited remarkable decolorization abilities, achieving 85% and 80% conversion after 180 min, respectively.

Notably, the Cu/clay catalyst proved to be a strong oxidizing agent, leading to complete

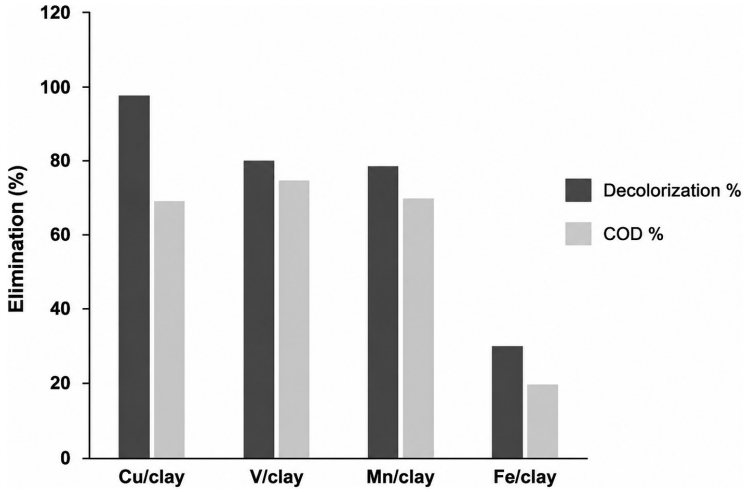

Figure 9. Effect of different catalysts on MO decolorization and COD removal ([MO]₀ = 4.6 × 10^{-5} mol L^{-1}; H_2O_2 = 2.5 mL; t = 120 min; pH₀ = 6.5; catalyst = 200 mg; metal loading = 5 wt.%)

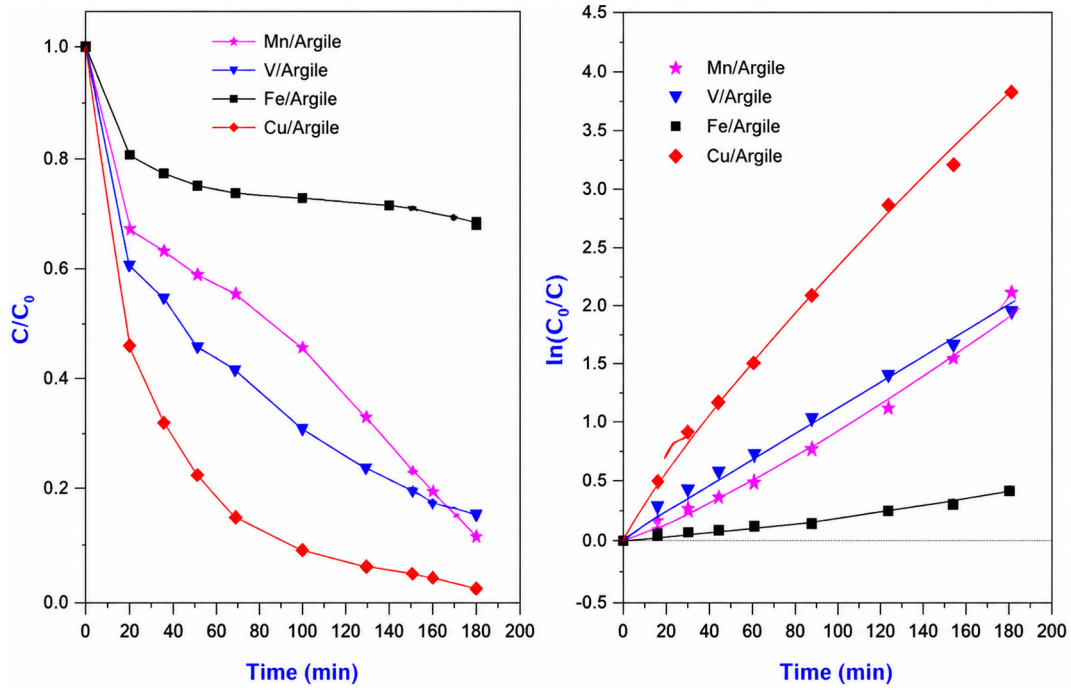

Figure 10. (a) Evolution of C_t/C_0 over time for 5% Cu/Clay, 5% V/Clay, 5% Mn/Clay, and 5% Fe/Clay catalysts; (b) evolution of ln (C_0/C_t) for the same catalysts under identical conditions (initial concentration: 15 mg/L; reaction time: 120 min; initial pH_0: 6.5; catalyst dosage: 200 mg; H_2O_2: 2.5 mL)

decolorization within 120 min. This superior performance can be attributed to the unique redox habitats of copper ions, which catalyze nucleophilic substitution reactions (Saranya and Anilkumar, 2020). Du et al. (2024) reported that Cu_2^+ based Fenton-type catalysts produce hydroxyl radicals (HO-) capable of oxidizing organonnear-neutralsninnear-neutrals in near-medial aqueous medium. These observations suggest that the daytime catalytic Fenton catalysts are powerful conditions for Fenton orange.

In the standard, the reaction rates of MO decomposition in aqueous solution obtained using the heterogeneous Fenton technique under maximum conditions are well defined by the following pseudo-first-order equation:

$$ln(C_0/C_t) = A + Kt \quad (4)$$

where: C_0 denotes the initial dye concentration, C_t the dye concentration at time t, t the decolorization time (min), K the apparent first-order rate constant (min^{-1}), and A an empirical constant derived from experimental fitting.

Kinetic analysis of methyl orange decolorization demonstrated that the process followed a pseudo-first-order model, with excellent agreement between the experimental data and the proposed equation. The fitted results based on the dataset are illustrated in Figure 10(A) is displayed in Figure 10(B), where the correlation coefficients (R = 0.979, 0.976, and 0.9803) for the Cu/Clay, V/Clay, and Mn/Clay catalysts were close to unity, confirming the validity of the kinetic model in all cases. Furthermore, the Cu/Clay catalyst exhibited the highest rate constant, indicating its superior catalytic efficiency in promoting the oxidative degradation of the dye compared to that of the other catalysts (Azimi et al., 2020).

Catalytic reusability

From the present experimental data, it can be concluded that the catalysts retained their activity for the oxidation of methyl orange at neutral pH and room (or ambient) temperature. The stability and recyclability of catalysts are crucial from both economic and environmental standpoints, and their reuse is expected to reduce the operating costs of wastewater treatment processes (Xu and Liu, 2023).

The catalyst was employed over three consecutive cycles using fresh dye solutions under the optimized conditions. At the end of each cycle, the catalyst was washed thrice with ultrapure water and dried in an oven at 100 °C. The recovered catalyst was subsequently reused in the next oxidation cycle.

As shown in Table 1, the catalysts were efficiently recycled in minimal cycles without any significant decrease in catalytic performance; however, a marked decrease in performance was observed over three cycles. All experiments were conducted at a fixed reaction time of 60 min, unless otherwise specified. Therefore, the catalysts exhibited good operational stability and could be reused without significant loss of catalytic activity.

Table 1. Decolorization efficiency of MO dye by the catalysts in three cycles

Number of cycles			
Catalyst	1st Cycle	2nd Cycle	3rd Cycle
Cu/Clay	92%	86%	71%
V/Clay	64%	41%	43%
Mn/Clay	62%	52%	52%
Fe/Clay	26%	29%	24%

CONCLUSIONS

This study demonstrates that supported clay-based catalysts prepared through impregnation with transition metals (Cu, V, Mn, and Fe) are remarkably effective in promoting the Fenton-type decomposition of the azo dye methyl orange using H_2O_2 as the oxide. The overall performance of the catalyst was shown to be strongly influenced by the nature of the metal, its dispersion in the support, and the subsequent morphology, with copper-based catalysts showing a very good last interest tool for each decolorization and COD removal under moderate conditions (natural pH and ambient temperature). with 2.5 mL H_2O_2 on Cu/clay (4 g/L) basis, completed almost complete (99%) decolorization of methyl orange in 180 min, revealing its potential in real-world applications in wastewater treatment to explain the nature of active copper network also understand the reaction mechanism of the hetero-oxidation process in general.

REFERENCES

1. Abdikamalova, A., Mamataliyev, N., Eshmetov, I., Kalbaev, A., Seytnazarova, O. (2024). Catalytic activity of iron-intercalated montmorillonites in the oxidation of dyes. *Conference Proceeding.* https://doi.org/10.1117/12.3017754
2. Azimi, S., Shirini, F., Pendashteh, A. (2020). Advanced oxidation process as a green technology for dyes removal from wastewater: A review. *Iranian Journal of Chemistry & Chemical Engineering-International English Edition*. https://doi.org/10.30492/ijcce.2020.43234
3. Azimi, S., Shirini, F., Pendashteh, A. (2020). Advanced oxidation process as a green technology for dyes removal from wastewater: A review. *Iranian Journal of Chemistry & Chemical Engineering-International English Edition*. https://doi.org/10.30492/ijcce.2020.43234
4. Biswal, S., Ranjan, C. (2025). Oxygen reduction reaction on Mn-doped Cu oxide electrodes. In

ChemRxiv. *American Chemical Society*. https://doi.org/10.26434/chemrxiv-2025-j4d6s

5. Chen, Y., Miller, C. J., Waite, T. D. (2021). pH dependence of hydroxyl radical, ferryl, and/or ferric peroxo species generation in the heterogeneous Fenton process. *Environmental Science & Technology*, *56*(2), 1278–1288. https://doi.org/10.1021/acs.est.1c05722
6. Contreras Olivares, N., Díaz-Nava, M. C., Solache-Ríos, M. (2016). Enhanced decolorization of dyes by an iron modified clay and thermodynamic parameters. *Water Science and Technology, 73*(8), 2007–2016. https://doi.org/10.2166/wst.2016.038
7. Diya'uddeen, B.H., Abdul Aziz A.R., and Daud, W.M.A.W. (2012). On the limitation of Fenton oxidation operational parameters: A review. *International Journal of Chemical Reactor Engineering*, *10*(1). https://doi.org/10.1515/1542-6580.2913
8. Du, H., Hu, X., Huang, Y., Bai, Y., Fei, Y., Gao, M., Li, Z. (2024). A review of copper-based Fenton reactions for the removal of organic pollutants from wastewater over the last decade: different reaction systems. *Environmental Science and Pollution Research International*, *31*(19), 27609–27633. https://doi.org/10.1007/s11356-024-33220-1
9. Duchesne, M. A., Nakano, J., Hu, Y., Maclennan, A., Hughes, R. W., Bennett, J., Nakano, A. (2016). *Vanadium Oxidation State Determination by X-Ray Absorption Spectroscopy* (pp. 1405–1412). Springer. https://doi.org/10.1007/978-3-319-48769-4_153
10. Enami, S., Sakamoto, Y., Colussi, A. J. (2013). Fenton chemistry at aqueous interfaces. *Proceedings of the National Academy of Sciences*, *111*(2), 623–628.https://doi.org/10.1073/pnas.1314885111 Hess, C. (2021). *Vibrational Spectroscopies*. 483–511.https://doi.org/10.1002/9781119436782.ch13
11. Gaibnazarov BB. Tursunov M.A., Tajibaev A.T., Khojiev Sh.T., Kosimov I.O. (2023). Reversible medium for recording and storing information based on vanadium dioxide v2o5. *Zenodo (CERN European Organization for Nuclear Research)*. https://doi.org/10.5281/zenodo.7541666
12. Hutchings, G. J. (2021). Spiers memorial lecture: Understanding reaction mechanisms in heterogeneously catalysed reactions. *Faraday Discussions*, *229*(0), 9–34. https://doi.org/10.1039/d1fd00023c
13. Ichikawa, S., Nakamura, T. (2023). Solid sample preparations and applications for x-ray fluorescence analysis. *Encyclopedia of Analytical Chemistry*, 1–24. https://doi.org/10.1002/9780470027318.a9562.pub2
14. Isibor, P. O., Imoobe, T. O. (2025). Principles of ecotoxicology in aquatic systems (pp. 18–31). *Pollution Tolerance of Freshwater Ecosystems and Biomonitoring* Crc. https://doi.org/10.1201/9781003647966-2
15. Jatoi, A. S., Hashmi, Z., Mubarak, N. M., Karri, R. R. (2023). Heterogeneous Advanced Oxidation Process (pp. 47–64). *Advanced Oxidation Processes for Micropollutant Remediation*. Crc. https://doi.org/10.1201/9781003247913-3
16. Kloprogge, J. T., Ponce, C. P., Ortillo, D. O. (2021). X-ray photoelectron spectroscopic study of some organic and inorganic modified clay minerals. *Materials*, *14*(23), 7115. https://doi.org/10.3390/ma14237115
17. Lamrani, M., Mouchane, M., Taybi, H., Mouadili, A. (2026). Physical and chemical characteristics of wastewater from the Fez industrial sector in Morocco. *BIO Web of Conferences, 212*, 01025. https://doi.org/10.1051/bioconf/202621201025
18. Leifert, D., Studer, A. (2019). The persistent radical effect in organic synthesis. *Angewandte Chemie International Edition*, *59*(1), 74–108. https://doi.org/10.1002/anie.201903726
19. Mancipe, S., Romanelli, G. P., Martinez, J. J., Luque, R. (2025). Formation of hydroxyl radicals in advanced oxidation processes for the degradation of contaminated organic matter. *Current Green Chemistry*, *12*(2), 117–137. https://doi.org/10.2174/0122133461335923240918061714
20. Marouf, R., Dali, N., Boudouara, N., Ouadjenia, F., Zahaf, F. (2021). Study of adsorption properties of bentonite clay. *Intechopen.* https://doi.org/10.5772/intechopen.96524
21. Mccann, S. D., Stahl, S. S. (2015). Copper-catalyzed aerobic oxidations of organic molecules: Pathways for two-electron oxidation with a four-electron oxidant and a one-electron redox-active catalyst. *Accounts of Chemical Research*, *48*(6), 1756–1766. https://doi.org/10.1021/acs.accounts.5b00060.
22. Minyukova, T. P., Khassin, A. A., Yurieva, T. M. (2018). Controlling the catalytic properties of copper-containing oxide catalysts. *Kinetics and Catalysis*, *59*(1), 112–122. https://doi.org/10.1134/s0023158418010081
23. Oh, H., Choi, S., Kim, J. Y., Ahn, H. S., Hong, S. (2019). Stoichiometric and electrocatalytic production of hydrogen peroxide driven by a water-soluble copper(ii) complex. *Chemical Communications, 55*(84), 12659–12662. https://doi.org/10.1039/c9cc06956a
24. Pareek, P., Ledwani, L. (2022). *Synthesis and Applications of Polymer–Nano Clay Composites in Wastewater Treatment: A Review* (pp. 237–256). Springer. https://doi.org/10.1007/978-3-030-98202-7_9
25. Pędziwiatr, P., Mikołajczyk, F., Zawadzki, D., Mikołajczyk, K., Bedka, A. (2018). Decomposition of hydrogen peroxide - kinetics and review of chosen catalysts. *Acta Innovations*, *26*, 45–52. https://doi.org/10.32933/actainnovations.26.5
26. Pessoa, E. G. (2025). *Conventional treatment in*

the removal of microcontaminants. Seven Editora. https://doi.org/10.56238/sevened2024.018-007

27. Pliego, G., Zazo, J. A., Garcia-Muñoz, P., Munoz, M., Casas, J. A., Rodriguez, J. J. (2015). Trends in the intensification of the fenton process for wastewater treatment: An overview. *Critical Reviews in Environmental Science and Technology*, *45*(24), 2611–2692. https://doi.org/10.1080/10643389.2015.1025646
28. Rajesh Ch, L., Rao N, M. (2022). Structural and optical properties of copper indium oxide nanocrystalline powders prepared by solid-state reaction method. *Journal of Nano- and Electronic Physics*, *14*(6), 06017–5. https://doi.org/10.21272/jnep.14(6).06017
29. Raza, M. A., Farwa, U., Mumtaz, M. W., Mukhtar, H., Rashid, U. (2023). *Homogeneous Advanced Oxidation Processes* (pp. 13–45). Crc. https://doi.org/10.1201/9781003247913-2
30. Ros, E. O. (2021). Hydrogen peroxide: A novel mechanism of its production from pure water. *Reactive Oxygen Species*, *11*. https://doi.org/10.20455/ros.2021.n.801
31. Saranya, S., Anilkumar, G. (2020). Copper Catalysis. In: *Copper Catalysis in Organic Synthesis*. Wiley, 1–5. https://doi.org/10.1002/9783527826445.ch1
32. Shindhal, T., Rakholiya, P., Varjani, S., Pandey, A., Ngo, H. H., Guo, W., Ng, H. Y., Taherzadeh, M. J. (2020). A critical review on advances in the practices and perspectives for the treatment of dye industry wastewater. *Bioengineered, 12*(1), 70–87. https://doi.org/10.1080/21655979.2020.1863034
33. Sun, B., Li, H., Li, X., Liu, X., Zhang, C., Xu, H., Zhao, X. S. (2018). Degradation of organic dyes over Fenton-like Cu_2O–Cu/C catalysts. *Industrial & Engineering Chemistry Research*, *57*(42), 14011–14021. https://doi.org/10.1021/acs.iecr.8b02697
34. Sun, M., Chu, C., Geng, F., Lu, X., Qu, J., Crittenden, J., Elimelech, M., Kim, J.-H. (2018). Reinventing Fenton chemistry: Iron oxychloride nanosheet for pH-insensitive H_2O_2 activation. *Environmental Science & Technology Letters, 5*(3), 186–191. https://doi.org/10.1021/acs.estlett.8b00065
35. Vaiano, V., De Marco, I. (2023). Removal of azo dyes from wastewater through heterogeneous photocatalysis and supercritical water oxidation. *Separations, 10*(4), 230. https://doi.org/10.3390/separations10040230
36. Van Groeningen, N., Thomasarrigo, L. K., Byrne, J. M., Kappler, A., Christl, I., Kretzschmar, R. (2020). Interactions of ferrous iron with clay mineral surfaces during sorption and subsequent oxidation. *Environmental Science: Processes & Impacts*, *22*(6), 1355–1367. https://doi.org/10.1039/d0em00063a
37. Xu, H., Liu, Y. (2023). New insights into novel catalysts for treatment of pollutants in wastewater. *Catalysts*, *13*(5), 840. https://doi.org/10.3390/catal13050840
38. Yang, R., Yang, H. (2022). Degradation of 4-chlorophenol through activating oxidants byzero-valent Al/Fe-saturated attapulgite composites. *SCIENTIA SINICA Chimica, 52*(7), 1156–1177. https://doi.org/10.1360/ssc-2022-0066
39. Yanping, G., Dahlina Bt Rusli, D. R. (2024). Application and prospect of ecological dyeing technology in clothing manufacturing. *International Journal of Research and Innovation in Social Science, 8*(8), 2141–2148. https://doi.org/10.47772/ijriss.2024.8080158